J. Geophys. 42, 561 – 580, 1977

Journal of Geophysics

A Survey on Initial Results of the Helios Plasma Experiment

H. Rosenbauer, R. Schwenn, E. Marsch, B. Meyer, H. Miggenrieder, M.D. Montgomery*, K.H. Mühlhäuser, W. Pilipp, W. Voges and S.M. Zink**

Max-Planck-Institut für Physik und Astrophysik, Institut für extraterrestrische Physik, D-8046 Garching bei München, Federal Republic of Germany

Abstract. The evaluation of plasma particle data of the prime mission (140 days past launch) of HELIOS-1 yielded new evidence about many aspects of the solar wind between 0.3 and 1 AU.

In contrast to current models, the leading edges of fast streams appear steeper at 0.3 than at 1 AU. The sharp boundaries with large angular gradients of bulk velocity which obviously separate fast streams on all sides from slow plasma near 0.3 AU, suggest different acceleration processes for slow and fast stream plasma with no intermediate stages. This idea is supported by a statistical study which shows that the observed bulk speed histograms are roughly bi-modal with a clear minimum between the low speed and the high speed plasma regimes. The internal states of the two regimes are also different and develop differently between 0.3 and 1 AU.

Strong radial gradients could be observed in the proton temperature of fast stream plasma, the electron temperature, the heat flux conducted by the electrons and the interplanetary potential as derived from the electron measurements.

Predominantly in fast streams, the electron distribution is often strongly skewed due to medium energy (30 to 300 eV) electrons flowing away from the sun along the magnetic field lines. This feature has been named "strahl". It is possibly indicative of plasma conditions similar to those assumed by exospheric theory.

Key words: Solar wind – Solar wind protons – Solar wind electrons – Fast stream boundaries – International states of fast and slow solar wind – Proton double streams – Radial gradients of the solar wind between 0.3 and 1 AU.

1. Introduction

On December 10, 1974 HELIOS A (after launch named HELIOS-1) was launched into an ecliptic orbit around the sun with a perihelion of 0.309 AU.

* Now with Los Alamos Scientific Laboratory

** Contributed to this paper while on a MPG fellowship at this institute

A slightly closer approach to the sun (0.290 AU) was achieved by means of the nearly identical spacecraft HELIOS B (after launch named HELIOS-2) which was launched on January 15, 1975.

This mission provided opportunities for the first in situ investigations of the interplanetary medium inside the orbit of Mercury and for novel measurements in the region between the orbits of the earth and Mercury.

The payloads of HELIOS-1 and 2 are also essentially identical. Of 10 experiments aboard, 8 are dedicated to the investigation of particles and fields in the interplanetary medium. (The spacecraft and all experiments are briefly described in a special issue of Raumfahrtforschung, **19**, 5, 1975).

This paper is intended to give a survey of the available main results of the HELIOS plasma experiment.

Most of theses results are based on the data obtained during the primary mission (140 days past launch) of HELIOS-1. During that time the data recovery rate was exceptionally high and the sun was very quiet. Therefore, this time interval appeared especially suitable for all kinds of analyses requiring complete sets of data and comparatively stationary conditions in the solar corona.

2. Spacecraft Characteristics Relevant to the Plasma Experiment

Both HELIOS probes are spin stabilized at 60 rpm with their spin axes perpendicular to the ecliptic. The rotation is used by the plasma instruments to measure the distribution of particle flow directions in spin angle.

The spin vector of HELIOS-1 is pointing toward the north pole of the ecliptic, whereas that of HELIOS-2 is pointing south. This difference in spin direction, assuming identical spacecraft and instruments, allows a check of a possible bias in the determination of the average azimuthal plasma flow angle.

The shape and surface characteristics of a spacecraft together with the momentary plasma conditions and the flux of UV photons determine the size and topology of the electric fields near the instrument apertures. These fields may accelerate, decelerate or deflect the low energy particles to be measured. The main body of each HELIOS spacecraft is a regular sixteen sided polygon in cross section. To both ends solar generators of inverted frustrum-shape are attached, giving the spacecraft a yarn spool-like appearence. Except for the four radial booms and the despun antenna, the whole probe is cylindrically symmetric about its spin axis. This is important since in only this way can the spin modulation of the spacecraft potential be minimized. The surface characteristics of HELIOS, as initially designed, were not favorable for low energy plasma measurements. Most of the sun lit areas were electrically insulating (quartz glass) and for areas in shadow (the interior of the solar generators) both insulating and conducting surfaces materials were to be used. Therefore, a programm for "electrostatic cleanliness" of the spacecraft was initiated, resulting in major improvements. Essentially all surfaces in the solar generators were made conductive. The final goal of covering all glasses on the solar cells and the "second surface mirrors" with a transparent conductive coating was not

achieved for cost reasons. However, a "belly-band" of approximately 30 cm width around the middle of the main compartment could be equipped with conductively coated second surface mirrors which were all electrically connected to the spacecraft structure. In this way, a sufficiently large photo electron emitting area was provided to keep the spacecraft potential slightly positive and the spacecraft surface surrounding the apertures of the instruments an equipotential.

The spacecraft transmits data to the earth with bit rates varying between 2048 bps and 8 bps. Depending on the measurement mode, a fraction of 10 to 35% of this data flux is allocated to the plasma experiment. During black-out times, or when no ground stations are available, data (at a very low bit rate) can still be recovered due to an on-board 0.5 megabit core memory, which is otherwise used for storage of fast transients measured by magnetic field and the plasma wave experiments.

3. Instrumentation

The HELIOS plasma experiment consists of 4 instruments (Schwenn et al., 1975). The three-dimensional ion analyzer (I 1a) employs a narrow quadrispherical electrostatic deflector ($R/\Delta R=60$) for particle analysis with respect to energy per charge (E/q) in 32 channels exponentially distributed between 155 V and 15.3 kV. Continuous electron multipliers (CEMs) in counting mode are used for particle detection. By means of 9 separate CEMs, angular resolution in 9 channels 5° apart is achieved in spacecraft polar angle (ε).

The direction of incidence of the particles with respect to the spacecraft spin angle (φ) is measured with the same resolution in 16 channels by making use of the spacecraft's rotation and sun sensor information. All measurement channels are nearly adjacent to each other in velocity space, but do not overlap.

The resolution in φ and E/q can be doubled at times of sufficiently stationary plasma conditions since the φ and the E/q channels are every other measurement cycle shifted electronically into the gaps between the normal channels.

Every spacecraft revolution the particle flow direction at a fixed E/q level is determined in a two-dimensional grid. A full 3-dimensional ion spectrum is measured every 40 s as long as the total data transmission rate of the spacecraft is equal or above 256 bps. For economic use of the data rate available, the instrument can be operated in an automatic peak tracing mode. In this mode, 3-dimensionally resolved results are transmitted only from the region in velocity space occupied by the proton and the α-distributions.

Instead of I 1a, the mass spectrometer I 3 can be operated. This instrument uses a novel type of electrodynamic analyzer for velocity (v) analysis of the ions at a selectable mass per charge (m/q) ratio. Otherwise it operates very similarly to I 1a. It likewise resolves particle distributions in three dimensions and follows a nearly identical data aquisition scheme. This instrument has the advantage of separating the distribution functions of protons and α-particles completely. Its drawbacks as compared to I 1a are smaller sensitivity and larger power consumption which restrict its use to times when the spacecraft is inside 0.6 AU.

The third instrument dedicated to ion measurements, I 1b, is much less sophisticated than I 1a and I 3 respectively. Instrument 1b is always operated simultaneously with either of these instruments. A hemispherical electrostatic analyzer ($R/\Delta R = 12$) is used for E/q analysis and a very sensitive electrometer (noise level $\approx 2 \cdot 10^{-16}$ A) for current measurement. This instrument integrates over both φ and ε angles and therefore delivers E/q current spectra only. From a comparison of results of I 1b with those of I 1a and I 3 respectively the ionization state of the measured ions can be derived, due to the different particle detection principles used in these instruments (Grünwaldt, 1976).

The electron instrument, I 2, is distinguished from previously flown electron instruments by special design features which eliminate disturbances from photoelectrons produced inside the experiment (Rosenbauer, 1973). These measures were so successful that no disturbance is noticable even in the lowest energy channels and when the instrument is viewing the sun directly. The energy range of the instrument extends from 0.5 eV to 1.66 keV. The field of view is less than 10×10 degrees wide and scans the plane of the ecliptic in 8 equally distributed channels. (In the HELIOS-2 instrument the angular channels are shifted by 22.5° every other measurement cycle such that the angular resolution can be doubled if two subsequently acquired spectra are merged together). In this way, the electron velocity distribution can be determined in a plane cutting through the distribution close to its center.

All plasma instruments on HELIOS-1 and HELIOS-2 have been working without any malfunction until the time of this writing. Only on HELIOS-1 some interference from the spacecraft was experienced. The noise level of the electrometer instrument was increased compared to ground tests because of mechanical vibrations produced by the bearing of the despun antenna. This effect could be completely omitted on HELIOS-2 by reducing the sensitivity of the instrument to microphoning. During the prime mission of HELIOS-1 the electron experiment was heavily disturbed everytime the high gain transmitting antenna on the spacecraft was used. Ground tests revealed that this disturbance was caused by a resonant electron multiplication effect in the antenna slots ("multipactor effect"). Fortunately, this disturbance disappeared after the first perihelion passage. For HELIOS-2 this problem was avoided by modification of the antenna.

4. Data Evaluation

The proton data presented in this paper have been evaluated by means of a computer routine which was developed for analysis of large quantities of data for survey purposes. To keep the program simple, a real three-dimensional analysis is replaced by the determination of three reduced, one-dimensional distribution in φ, ε, and v which are naturally resolved by the instruments 1a, and 3. These reduced distributions are obtained by suitable integrations over the remaining variables. To determine v from the E/q measurements of I 1a, the assumption is made that the largest hump of the distribution is due to protons.

After correction of dead-time effects and subtraction of background count rates the plasma velocity space density for each measurement channel is computed from the count rates and the zeroth moments of the instrument functions obtained form laboratory calibrations. The measurement channels are treated as δ-functions. Their positions in velocity space are determined from the first moments of the calibration results. An algorithm then limits the velocity space around the center of the proton distribution such that the main part of the α-distribution is no longer included in the further calculations. After a suitable interpolation between the phase space densities obtained in the grid of measurement channels, the zeroth, first and second moments of the distribution in three orthogonal directions (flow velocity unit vector, in and out of the ecliptic) are determined. Therefrom the bulk velocity vector, the temperatures in the three directions, and the number density are calculated. The I 1b results, which are one-dimensional anyway, are evaluated correspondingly with a similar routine. The orbital motion and the exact orientation of the spacecraft are taken into account for correcting the flow velocity. The evaluation of the electron data is much more sophisticated. A description of this routine would be beyond the scope of this paper.

The accuracy of the plasma parameters obtained this way could be checked by comparisons with parameters determined from both the Los Alamos and the MIT IMP 7/8 plasma experiments at times when the spacecraft were close together, and with plasma densities determined by the plasma wave experiment aboard HELIOS. The agreement was in all cases very satisfactory.

5. Proton Results

5.1. The Status of the Corona and the Interplanetary Plasma During the Primary Mission of HELIOS-1

As typical of the time close to solar minimum, the sun was very "quiet" during the period of December 1974 through April 1975. Only minor flare activity was reported, and only two major interplanetary shock waves generated by flares could be measured by HELIOS-1 (January 6 and 8, 1975). Otherwise, the large scale conditions in the corona were quite stationary. The corona observations at that time (Sheeley et al., 1976; Schwenn et al., 1976) show large coronal holes over the polar region extending close to or beyond the solar equator at two positions (Around Carrington longitude 120° and 270° respectively). Two exceptionally pronounced and long-lived fast streams in the solar wind, which had been observed from earth orbiting spacecraft for several previous solar rotations (Bame et al., 1976), still prevailed during the observation period discussed here.

Velocity, density and radial temperature (1-hour averages) as measured by HELIOS-1 are plotted versus Carrington longitude in Figure 1. The heliographic latitude of the spacecraft, its distance from the sun and the time of observation in days of the year are also indicated along the abscissa. The two corotating fast streams are easily recognized. The change that seems to occur between

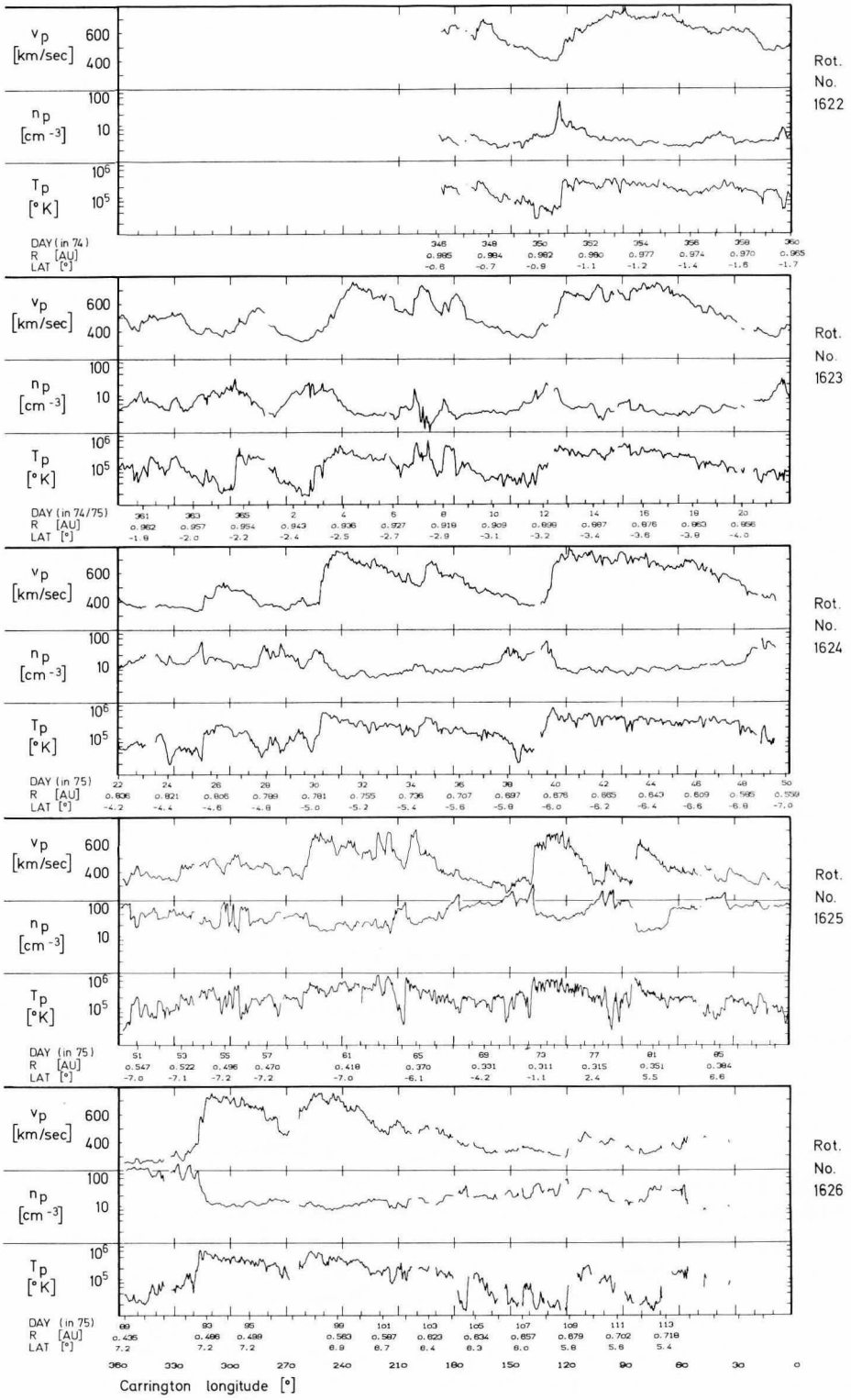

Fig. 1. One hour averages of solar wind proton bulk speed, number density and radial temperature versus Carrington longitude, as measured by HELIOS-1 between December 12, 1974 and April 25, 1975. The time of measurement and the radial distance and solar latitude of the spacecraft are also indicated along the abscissa

rotations 1624 and 1626 (panels 3 and 5) can mainly be attributed to causes other than temporal changes in the source region (see section 5.2). By comparison with IMP 7/8 data (Los Alamos) it could be confirmed, that the general stream structure was stationary also through rotations 1625 and 1626.

5.2. Fast Stream Structures Between 0.3 and 1 AU

In this section, only the velocity, density and temperature profiles of fast streams and their typical changes between 0.3 and 1 AU shall be regarded. The development of the internal state of the plasma in fast streams as compared to slow plasma is discussed in section 5.3 of this paper.

If we first regard the proton bulk velocity profiles in the upper four panels of Figure 1 we notice as the most striking feature the steepening of the leading edges of the fast streams, as HELIOS approaches the sun. This result was quite unexpected, since model calculations (Hundhausen, 1973; Pizzo and Hundhausen, 1976; Durney and Pneuman, 1975) predict the opposite: a continuous steepening of the fronts of the velocity profiles with increasing distance from the sun until a shock forms.

With respect to the trailing edges of the fast streams, the observations are in qualitative agreement with the present models. An increase of the angular speed gradients with decreasing distance from the sun should be expected there. This is most clearly seen if we do not regard the bulk speed profile alone, but also temperature and number density. A comparison between panels 1 and 3 of the large fast stream observed between approximately Carrington longitude 120° and 20° shows that all parameter profiles tend to change toward mesa-like structures (or inverse-mesa structures respectively) with sharp leading and relatively sharp trailing edges, as HELIOS travels from 1 AU to 0.6 AU. A decline in velocity faster than ever observed near 1 AU, from 650 km s^{-1} to 300 km s^{-2} in only about 20° heliographic longitude, can also be seen in panel 4 around Carrington longitude 110° where HELIOS is at a heliocentric distance of 0.31 AU.

Until now, the terms "leading" and "trailing" edges of fast streams, common in the respective literature, have been used. It must be noted, however, that these terms can be misleading in so far as they primarily describe the time sequence of observations. They give a correct notion of the spatial shape of a fast stream only if the transition fronts observed are essentially north-south oriented. In principle, it could happen, however, that a separation surface between fast and slow plasma, which is merely east-west-ward oriented in a heliographic coordinate system, is crossed by an observing spacecraft. In such a case, the terms "leading" or "trailing" edge obviously loose their sense, and the physical interpretation must take this into account. Most likely, such cases are not so rare at all. Several similar situations have been observed by HELIOS.

If we compare panels 3, 4 and 5, it seems as if large temporal changes on the sun had occurred, because the second fast stream appears interrupted several times in panel 4 and is completely gone in panel 5, whereas a "new"

stream shows up around Carrington longitude 315° in panel 5. Comparisons with IMP-data taken near 1 AU, which show no drastic changes in the stream structures confirm, however, that the conditions in the source region actually have been stationary to a large extent. For resolving the seeming discrepancy, we must note that HELIOS-1 (in contrast to IMP 7/8) traveled from a heliographic latitude of $-7.25°$ to $+7°$ during solar rotation 1625 depicted in panel 4. Obviously HELIOS moved several times in and out through the northern boundary of the fast stream between $-1°$ and $+5°$ heliographic latitude (panel 4) and saw nearly no indication of a fast stream during the next solar rotation at the same position in heliographic longitude at a latitude of $+5.5°$ (Schwenn et al., 1976). Similar considerations hold true for the "new" stream around 300° Carrington longitude in panel 4. These observations, together with the flow angle measurements, which indicate a nearly radial flow between 0.3 and 1 AU, prove that fast streams have boundaries in heliographic latitude only a few degrees wide (Schwenn et al., 1976). The measurements further imply that probably most boundaries are not crossed in the direction of the real gradients but rather under a large oblique angle. Therefore, the observed angular gradients are only lower limits to the real values.

Summarizing our observations of "leading", "trailing" and "latitudinal" boundaries, we conclude that fast streams near 0.3 AU exhibit sharp boundaries in all directions. This finding, taken together with the observation of mesa-like profiles of large fast streams near 0.3 AU, implies that possibly because of new critical points developing in highly diverging flows (Kopp and Holzer, 1976), solar wind emerges from the corona in two different states, a "fast" and a "slow" one. This idea will be followed up in section 5.3 of this paper.

The apparent decrease of angular velocity gradients at the boundaries of fast streams with increasing distance from the sun might in the case of predominantly north-south ward oriented separation surfaces be caused by interaction regions growing in thickness with increasing distance from the sun due to a high magnetosonic speed. In the case of essentially east-west ward directed separation surfaces most likely quasi-viscous interactions between the fast and slow streams slipping along each other must be invoked. Several processes can be imagined which could accomplish the deep-reaching momentum exchange necessary to flatten the transitions as observed. Large scale hydrodynamic turbulence might develop, hydromagnetic waves refracted from the fast into the slow stream and accelerating the plasma there might play a role, waves generated by the velocity gradients might act similarly, and also mutual penetration of streams of different speed (Feldman et al., 1974) might be important. It must be kept in mind, however, that HELIOS moves much faster in heliographic latitude close to the sun than at larger heliocentric distances. Therefore, merely east-west ward oriented interaction layers with constant latitudinal velocity gradients would seem to have decreasing angular velocity gradients with increasing distance from the sun.

The fact that fast streams do not as readily steepen and produce co-rotating shock waves as suggested by most model calculations may in, the light of the HELIOS observations, be due to the neglection of quasi-viscous interactions in the models or to the assumption of too low magnetosonic speeds. However,

most likely, in many cases the orientation of the separation surfaces in predominantly east-west rather than north-south direction plays a role as well.

5.3. Radial Gradients of Fast and Slow Solar Wind

The sharp transitions between fast and slow plasma streams and the mesa-like profiles of the fast streams observed inside 0.6 AU, as discussed in the above section, suggest that (at least) two different acceleration mechanisms for the solar wind might exist, one producing fast plasma, also characterized by low density, and another one producing slow and dense plasma. A statistical study carried out with all proton bulk speed measurements performed during four solar rotations supports this notion. The resulting histograms are shown in Figure 2. The range of heliocentric distances HELIOS-1 traversed during these measurements were 1 to 0.9 AU for panel 1 (top), 0.9 to 0.7 AU for panel 2, 0.7 to 0.35 AU for panel 3, and 0.3 to 0.65 AU for panel 4 (bottom).

All histograms are roughly double-humped with clear minima at about 600 km s^{-1} in panels 1 to 4, and 500 km s^{-1} respectively in panel 4. The minimum is most pronounced in panel 4, where the spacecraft is closest to the sun. Future studies based on all HELIOS solar wind measurements should reveal whether or not the details visible in the structures of the low speed peaks are significant.

For the further investigations, the data of each rotation were divided into two groups of slow and fast plasma respectively, according to the minima at the dashed lines in Figure 2. Significant differences between the slow and the fast plasma could be found in all parameters, including flow angels and electron parameters (see section 6.2). Only the density and proton temperature results shall be briefly discussed here.

The densities, normalized to 1 AU assuming radial flow and constant speed, and averaged over each rotation, are depicted in Figure 3 as bars over the range of the heliocentric distance which was coverd by HELIOS during the respective solar rotation. For clarity the results of the third rotation (corresponding to panel 3 in Figure 2) were removed, since the range of heliocentric distance did overlap with that of rotation 4. The results are indicated by hollow bars for slow plasma, by solid bars for fast plasma, and by dashed bars for the average of all results. The higher density of the slow plasma as compared to the fast plasma, obvious from Figure 3, is in qualitative accordance with all results obtained in the past and is therefore not surprising. The radial gradients, however, which can be derived from this figure appear interesting. It must be noted that no change of the normalized density with distance from the sun would mean that the plasma expands either according to the assumption made for normalizing the densities (radial flow at constant speed) or at least such that the product of the speed and the cross section of the flux tube remains constant. The fast plasma obviously behaves about like that. The decrease with heliocentric distance of the slow plasma density, however, indicates that this plasma either expands laterally or is significantly accelerated on its way between 0.3 and 1 AU.

In Figure 4, where the plasma temperatures are shown in a similar way

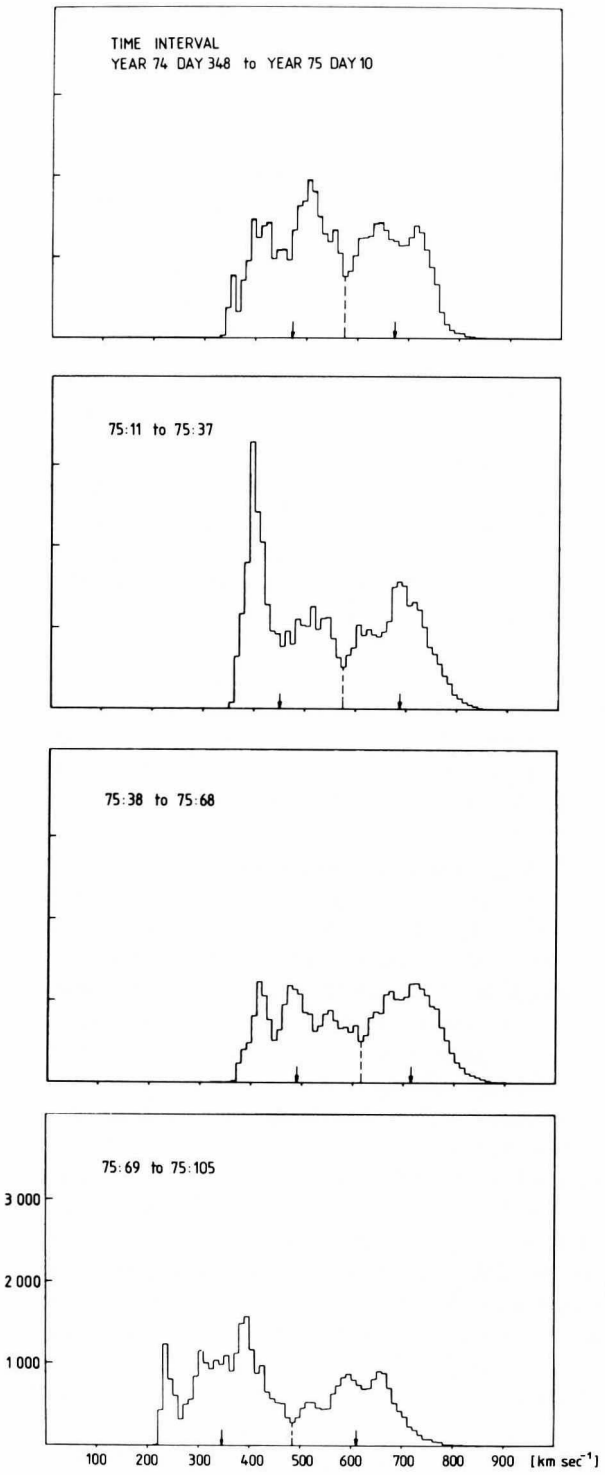

Fig. 2. Histograms of all solar wind proton bulk speed measurements performed by HELIOS-1 during four subsequent solar rotations. The minima between the two main humps of the distributions are marked by dashed lines. The mean values of the two regimes defined in this way are indicated by arrows. It shall be noted that corrections for non-uniform data coverage which would result in minor changes of the histograms have not yet been made

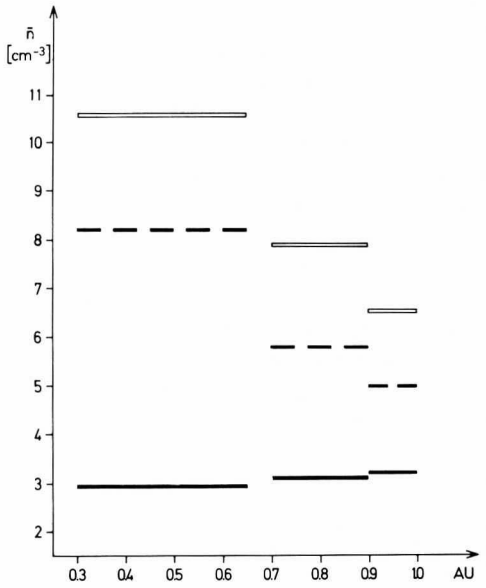

Fig. 3. Mean values of all proton number densities determined during solar rotations 4, 2 and 1 of Figure 2. The densities have been normalized to 1 AU assuming radial flow at constant speed. For each rotation the mean values have been calculated separately for (i) all results (dashed line); (ii) fast streams (solid line); (iii) slow plasma (hollow line). The dashed lines in Figure 2 have been chosen as the separations between fast and slow plasma

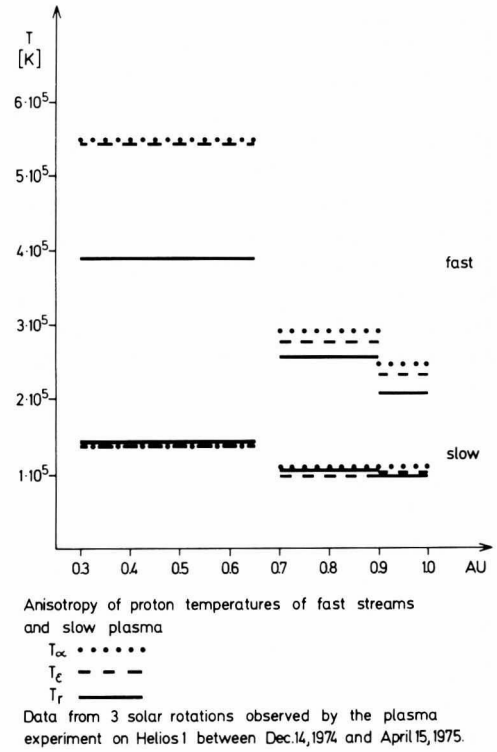

Fig. 4. Mean values of all proton temperatures measured during solar rotations 4, 2 and 1 of Figure 2. For each rotation the mean values of three proton temperatures have been calculated separately for fast (upper part of the figure) and slow plasma. The temperatures in the direction of the flow velocity are given in solid lines, the temperature in the perpendicular direction in the ecliptic in dotted lines and perpendicular to the ecliptic in dashed lines

as the densities in Figure 3 (however without normalization), again the radial gradients are most interesting.

The slow plasma seems to expand nearly isothermally, whereas the fast plasma cools down by about a factor of two between 0.45 AU (the average heliocentric distance of HELIOS during rotation 4) and 1 AU. These results are in qualitative accordance with the plasma expansion as derived from Figure 3. The indication in Figure 4 of a large anisotropy of the proton temperature in high speed streams close to the sun shall not be discussed in this paper.

We think that the observations of distinct differences between fast and slow plasma in both the size and the radial gradients of the most important plasma fluid parameters supports our notion that two different acceleration mechanisms (with a certain spread in the parameters of the plasma produced, but with no real intermediate stage) are responsible for the generation of slow and fast plasma respectively.

Therefore, we would like to briefly discuss some consequences of a hypothetic model with two different states of solar wind. The plasma parameters resulting form the assumed two different acceleration mechanisms should, to a first order approximation, not depend on the solar latitude or the (large scale) size or shape of the source regions.

All average latitudinal and temporal variations of solar wind parameters observed should then primarily be caused by differences in the mixture-ratios of "slow" and "fast" plasma. Essentially undisturbed plasma of both regimes should alternatively be observed if either the source regions of uniform nature are so large or the observations are made so close to the sun that the interaction zones can be neglected. Then, the slow and the fast plasma can be studied separately and e.g. radial gradients can be established, as done here, even without considering temporal changes in the source region or differences in the position of the spacecraft.

The fact that bi-modal speed histograms were only rarely found in the past (Gosling et al., 1976) does, in our opinion, not disprove our notion. Most of these observations were made during years of increased solar activity, where the coronal holes and the corresponding fast streams are known to be of smaller scale size (Bame et al., 1976). It must be expected that under these conditions the differences between the two plasma regimes, that may have existed close to the sun, have been smeared out by stream-stream interactions (see section 5.2) by the time the plasma reached 1 AU.

5.4. Separation of Proton Double Streams and α-Particles

Since it was first reported (Feldman et al., 1973) that the proton velocity distributions in the solar wind are often double humped along the magnetic field lines, this feature has attracted much attention and several models have been proposed for explaining this phenomenon (Montgomery et al., 1973, 1975, 1976; Feldman et al., 1973, 1974).

The evaluation of multiply peaked data is difficult if electrostatic (E/q) analysis is used alone, since a second high-energy hump of the proton distribution cannot be uniquely separated from the α-particle distribution. The HELIOS

plasma experiment improved the observational situation in several respects: the main instrument (I 1a) measures a three-dimensional particle distribution, whereas two-dimensional measurements had been used for this type of investigation in the past. A good resolution in all dimensions makes it easier to distiguish between an extension of the proton distribution along the magnetic field and an α-particle distribution displaced mainly in E/q. In addition, the charge state of questionable parts of the distribution can be checked by comparing the particle fluxes measured by I 1a (counting detector) with the simultaneously measured results of I 1b (electrometer detector). At times when the electrodynamic analyzer (I 3) is used instead of the main instrument, the data interpretation is no longer ambiguous at all. Since this instrument measures particle velocities with m/q as a parameter, the undisturbed three-dimensional velocity distribution of the protons can be studied.

The Figures 5 and 6 illustrate, that a second peak of the proton distribution can actually easily be mistaken for α-particles and vice versa, if only electrostatic

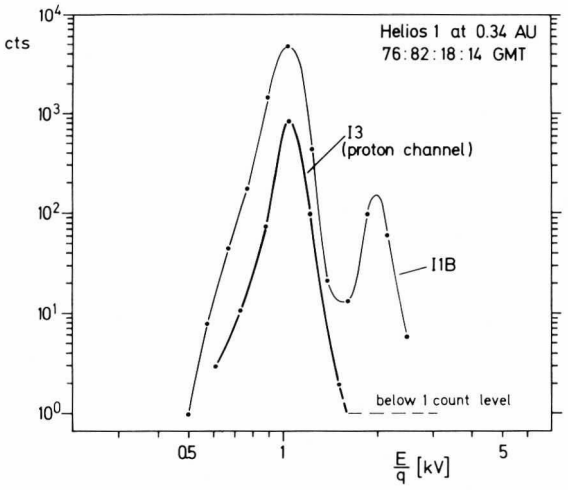

Fig. 5. Count rate spectra simultaneously measured by the electrodynamic analyzer (I 3) in the proton channel and the electrostatic analyzer (I 1b) (one "count" of the latter instrument corresponds to $1.6 \cdot 10^{-16}$ Cb). The second hump in the spectrum of I 1b must be due to ions other than protons, most likely α-particles

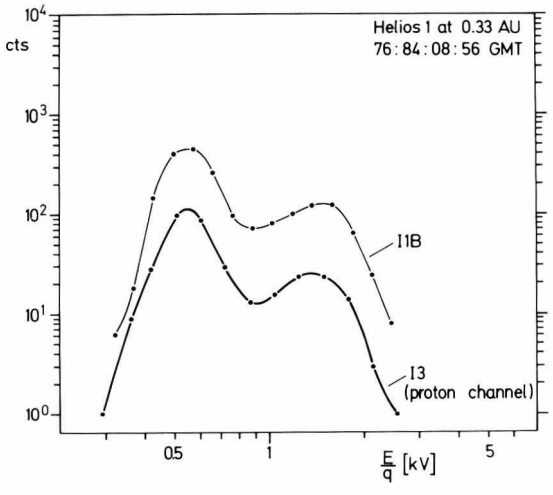

Fig. 6. Count rate spectra as in Figure 5. The second hump of the spectrum measured by I 3 is completely due to a fast stream of protons. The second hump of the I 1b-spectrum also indicates this fast stream, but may also contain α-particles

analyzers are used. One-dimensional count rate spectra obtained simultaneously from the electrodynamic analyzer (I 3) and the electrostatic electrometer instrument (I 1b) are displayed. Figure 5 shows the "normal" case where the second hump in the distribution measured by the electrostatic analyzer does not show up in the proton spectrum determined by the electrodynamic analyzer. In this case it must be concluded that the second hump was produced by an ion species other than protons, most likely α-particles. In contrast, Figure 6 shows a situation where the two instruments measure very similar double-humped distributions. That this kind of distribution is measured in the proton channel of the electrodynamic analyzer, proves that actually a double-stream proton distribution with large differential velocity is being observed. If only the results of the electrostatic instrument had been available, the second hump would most likely have been misinterpreted as being due to α-particles. This sheds some doubts on previous α-particle studies based on measurements of electrostatic analyzers, unless the magnetic field direction was carefully considered in the analysis.

6. Electron Results

6.1. The "Strahl" in the Electron Distribution

When the magnetic field vector lies in the scanning plane of the instrument, a pronounced skewness is often found in the medium energy range of the electron distribution indicating fast electrons streaming away from the sun along the magnetic field lines. This feature was named the "strahl"[1] and represents a new striking phenomenon in the solar wind electron distribution (Rosenbauer et al., 1976a; Miggenrieder et al., 1976) often clearly distinguishable from the "core" and the "halo" observed and defined earlier (Feldmann et al., 1975). An example of a distribution with a well developed strahl is given in Figure 7. A cut through the distribution in the scanning plane of the instrument (the ecliptic) is shown in terms of isodensity contours in velocity space. The coordinate system is centered in the maximum of the distribution. The v_x direction is toward the sun. The projection of the magnetic field direction, which was nearly parallel to the plane of observation at that time, is also indicated.

The strahl feature is clearly visible from the bulges of the density contours. It is also evident that these bulges represent electrons travelling away from the sun along magnetic field lines. The three-dimensional distribution function can be visualized as being symmetric about the magnetic field direction. It must be noted that the representation chosen here tends to deemphasize the strahl. Count rate spectra versus angle would show the strahl more clearly (see Rosenbauer et al., 1976a). As a contrast to Figure 7, a distribution without a strahl is shown in Figure 8.

[1] Earlier the word "beam" had been used as a translation of the German word "Strahl" (Rosenbauer et al., 1976a), however this word was found to carry too many connotations in plasma physics

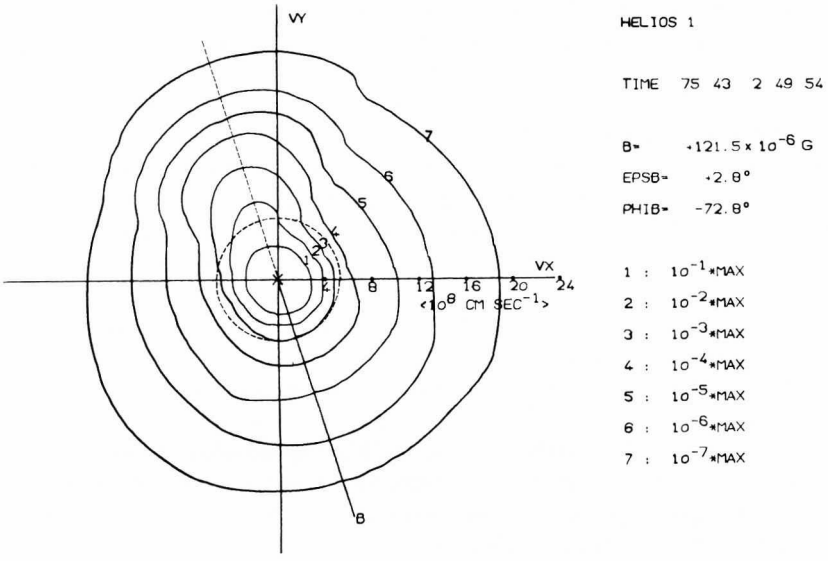

Fig. 7. A cut through a solar wind electron distribution exhibiting a "strahl". Isodensity contours in velocity space are plotted. The coordinate system is centered in the maximum of the distribution. The magnetic field direction is very close to the plane of observation. Its projection indicated in the figure appears as the line of symmetry. The mean thermal velocity is given as a dashed circle. The plasma bulk speed is 700 km s^{-1}, the number density 8.6 cm^{-3} and the distance to the sun 0.64 AU. Small details visible in the contours are artifacts of the plotting routine and should be disregarded, since the distance of the centers of angular measurement channels is 45°

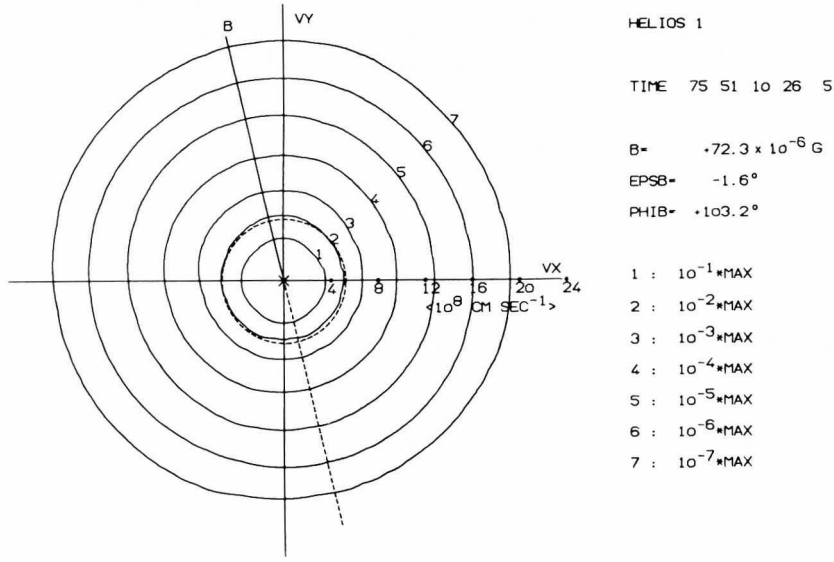

Fig. 8. The same display of an electron distribution as in Figure 9. Even though the magnetic field direction is again very close to the plane of observation, no strahl can be recognized. The plasma bulk speed is 370 km s^{-1}, the number density 66 cm^{-3} and the solar distance 0.54 AU

The strahl is characterized by the following main features:

– It is directed along the magnetic field away from the sun

– Its FWHM at medium energies (slightly above the energy separating core and halo) generally seems to be in the range between 30° and 120°. However, because of the coarse angular resolution of the instrument, it cannot be excluded that the strahl is much narrower at times. Further studies based on HELIOS-2 data with better angular resolution should give more accurate values.

– The clear break in the energy spectrum, which separates the core and the halo in all other directions than the strahl direction, is missing in the strahl.

– The slope of the distribution along the strahl direction decreases monotonically with energy. (No second peak).

– Any time a strahl is clearly developed, it carries the major part of the heat conduction.

– The strahl is predominantly observed in high speed solar wind streams.

We interpret the strahl as that part of the electron distribution which has travelled away from the corona to the point of observation without having undergone reflections or strong pitch angle scattering. The strahl population is in this way distinguished from the core electrons which, on the average, should have bounced several times between the retarding electrostatic potential at larger radial distances and the magnetic mirror closer to the sun (Feldman et al., 1975). The strahl's contrast with the halo probably results from the differing amounts of pitch angle scattering the particles in the two regimes have experienced.

Since a strahl-like feature in the electron distribution has been predicted by exospheric theory (Jockers, 1970), the presence of a strahl is likely to indicate conditions in the corona favoring the applicability of exospheric theory (low density, fast expansion). The fact that the strahl is generally more clearly developed in high speed streams could indicate that these conditions do often prevail in the source regions of fast streams (coronal holes) but only rarely in that part of the corona from which slow plasma is emerging.

Concluding this section, we would like to note that, by suggesting a name for a feature of the solar wind electron distribution which had been missed in the data analysis in the past, we do not want to emphasize the view of this feature as a uniquely identifiable "part" of the distribution that should be regarded separately. We rather find that all kinds of transitions between distributions as shown in Figures 7 and 8 can be observed. Since, however, a well developed strahl is such a prominent feature of the distribution and certainly is an indication of special, (not yet quite understood) physical conditions in the solar wind or its source region, it suggested itself to study this feature, name it and use it as a new ordering parameter in special studies.

6.2. Differences Between Fast Streams and Slow Plasma Manifested in the Electron Distributions

In order to attain a better ordering of electron parameters as a function of radial distance from the sun, it was necessary to consider fast and slow stream

data separately. The separation was achieved in the same way as described in section 5.3, but in addition compression regions between fast and slow plasma streams were removed. The following main differences between electron distributions in fast streams and in slow plasma respectively can be noted:

– The strahl is sometimes missing in fast streams and only rarely observed in slow plasma. (This is a revision of the statement made by Rosenbauer et al., 1976a, that the strahl is observed nearly all the time. This wrong notion resulted from an unfortunate selection of raw data at that early stage of analysis).

– The conducted heat flux is on the average higher in low speed plasma than in fast streams.

– The temperatures are found to be lower on the average in high speed streams than in slow plasma.

These results seem to support the conclusion drawn from the proton results that in all studies about radial variation fast streams and slow solar wind plasma must be treated separately. Obviously, not only the main plasma parameters, but also the processes contributing to plasma acceleration (as heat conduction), are largely different in these two parameter regimes.

6.3. Radial Gradients of Solar Wind Electron Parameters

Radial gradients of solar wind parameters are known to be often obscured by latitudinal gradients (Rhodes and Smith, 1975; Schwenn et al., 1976) and nonstationary conditions in the source regions.

In order to establish quantitative radial gradients, more data than analyzed by now must be available. Therefore, we only want to indicate the order of magnitude of some of the presently available results.

The largest changes with heliocentric distance r were found in the heat flux density w conducted by the electrons. Even though a power law of the form:

$$w = w_0 \left(\frac{r}{r_0}\right)^{-\alpha}$$

with α as large as 2 must be expected, if the conducted heat flux in a radially expanding flux tube would remain constant, the actually observed average values for α of the order of 4 appear rather large. The size of this empirical power law index implies that about 90% of the conductive energy supply available at 0.3 AU is transformed into other forms of energy between there and 1.0 AU. Further studies may reveal how this transformation is achieved and where the energy goes.

The radial gradient of most interest for comparison with different solar wind expansion theories is the one of the mean thermal energy of the electrons. Even though the fluctuations found are large, and therefore no final result can be given yet, it is clear that the extreme values as a $r^{-4/3}$ dependence required by an adiabatic one-fluid model can be ruled out as well as a $r^{-2/7}$ law expected for an expansion according to a two fluid model (for a review see e.g. Hundhausen, 1972).

If the break between the core and the halo of the electron distribution is interpreted as a measure for the local (positive) electrostatic potential with respect to infinity (Feldman et al., 1975) an increase of this potential with decreasing distance from the sun should be expected. Even though again the scatter of the results is large, such an increase could clearly be found. Near 1 AU the energy limit for the quasi-trapped particles of the core of the distribution is typically of the order 30 to 40 eV. At 0.3 AU that limit increases by roughly a factor of 3 on the average. That means that, on the average, ions would gain about 50 to 100 eV per unit charge and electrons would lose the same amount on their way between 0.3 and 1 AU if other processes, like e.g. momentum exchange between particles and direct momentum transfer from waves, could be neglected.

Conclusions

None of the topics touched in this summary paper could be dealt with in great detail. On most of the subjects, however, specific studies are under way which will be published soon. Even though some other studies have not yet proceeded so far that results could be reported, we hope that the HELIOS plasma measurements will yield contributions to many more questions than could be adressed here.

As far as the results reported here are concerned, it must be kept in mind that the statistical significance of the observations during the first approach of a HELIOS spacecraft to 0.3 AU is naturally limited.

It will certainly be necessary to critically review these results when longer periods of measurements have been evaluated. In adition, it must be emphasized that all data obtained, to date, by the HELIOS spacecraft are likely to be representative only of the time close to the solar minimum. The forthcoming time of increasing solar activity may well revise the current picture of the physical processes in the inner solar system provided by the HELIOS data.

Acknowledgements. At the occasion of publication of the first survey on the scientific results of the HELIOS plasma experiment, the authors would like to express their gratitude to the many individuals, organizations and companies who contributed to the success of the HELIOS mission and this experiment.

The HELIOS project was jointly conducted and supported by the German Bundesministerium für Forschung und Technologie (BMFT) and the National Aeronautics and Space Administration (NASA) of the USA. The HELIOS plasma experiment was supported by the BMFT under grant No. WRS 10/7. We would like to express our thanks to the German program scientist Dr. Otterbein, and to the program manager Mr. Käsmeier.

The German part of the project was managed by Mr. Kutzer and his assistant Dr. Unz (at the DFVLR-BPT, the former GfW), the US part by Mr. Ousley (NASA-Goddard Space Flight Center). We appreciate the good cooperation we had with all members of the team directly concerned with our experiment – Drs. Kasten, Wodsak, Dodeck, Stampfl, Kempe and Mr. Galle.

Our experiment was developed to flight-readiness and manufactured by Messerschmitt-Bölkow-Blohm GmbH (MBB) with contributions from the companies Lewicki, Zeiss and Dornier-System GmbH. The project manager Dr. Brauer, together with Mr. Wagner and Mr. Jochimsen, was responsible for mechanical design and fabrication. Messrs. Stiller, Friedrich, Nogai and their colleagues developed the sophisticated electronics. It is certainly largely due to the carefulness and

unusual personal involvement of all members of this group that our experiment is still working flawlessly in all respects. We also appreciate the diligent work of the MBB spacecraft team and especially the good cooperation we had with Messrs. Grün, Schuran, Ziegler and the spacecraft integration group. The NASA-KSC team carefully prepared and performed both HELIOS launches; NASA provided their deep space network ground stations for tracking. We would like to express our appreciation to Mr. Heftman at JPL for his continuous help and also to Prof. Hachenberg and his colleagues at the MPI für Radioastronomie for making the 100 m Effelsberg dish available for HELIOS data acquisition.

The DFVLR team at the German Space Operation Center (GSFC) headed by Mr. Panitz attentively performs mission operations. Valuable assistance was given by the NASA-JPL team. Now Mr. Kehr directs the HELIOS-mission, assisted mainly by Mr. Hiendlmayer and colleagues. We thank also Messrs. Wiegand, Piotrowski and Mrs. Dusl and others for their diligent work in preparing the experiment data tapes.

In our institute the experiment has been supported continuously through more than a decade by Profs. Lüst and Pinkau. Mr. Pellkofer, the first project manager, Messrs. Ludwig, Müller, Kaiser, Fischer and Mrs. Sckopke contributed to development, tests and calibration of the instruments for several years. Messrs. Antrack, Kipp and Ms. Lipp still assist us in data processing.

To all these persons and all the many others who could not be mentioned here we are deeply indebted. We also thank the project scientists Drs. Porsche, Meredith and Trainor for their continuous efforts in coordinating the interests of so many scientists. We gratefully acknowledge the magnetic field data provided to us by Prof. Neubauer (Technische Universität Braunschweig), and also the plasma data from the IMP 7/8-satellites made available to us by the groups at Los Alamos Scientific Laboratory and the Massachusetts Institute of Technology.

Finally we thank Dr. B. Feldman and Dr. J. Scudder for valuable discussions and Ms. Maier for typing the manuscript.

References

Bame, S.J., Asbridge, J.R., Feldman, W.C., Gosling, J.T.: Solar cycle evolution of high speed solar wind streams. Astrophys. J. **207**, 977–980, 1976

Durney, B.R., Pneuman, G.W.: Solar-interplanetary modelling: 3-D solar wind solutions in prescribed non-radial magnetic field geometries. Solar Phys. **40**, 461–485, 1975

Feldman, W.C., Asbridge, J.R., Bame, S.J., Montgomery, M.D.: Double ion streams in the solar wind. J. Geophys. Res. **78**, 2017–2027, 1973

Feldman, W.C., Asbridge, J.R., Bame, S.J., Montgomery, M.D.: Interpenetrating solar wind streams. Rev. Geophys. Space Phys. **12**, 715–723, 1974

Feldman, W.D., Asbridge, J.R., Bame, S.J., Montgomery, M.D., Gary, S.P.: Solar wind electrons. J. Geophys. Res. **80**, 4181–4196, 1975

Gosling, J.T., Asbridge, J.R., Bame, S.J., Feldman, W.C.: Solar wind speed variations. J. Geophys. Res. **81**, 5061–5070, 1976

Grünwaldt, H.: Solar wind composition from HEOS-2, S-210 plasma experiment. In: Space Research XVI. Berlin: Akademie-Verlag 1976

Hundhausen, A.J.: Coronal expansion and solar wind. Berlin-Heidelberg-New York: Springer 1972

Hundhausen, A.J.: Non-linear model of high-speed solar wind streams. J. Geophys. Res. **78**, 1528–1542, 1973

Jockers, K.: Solar wind models based on exospheric theories. Astron. Astrophys. **6**, 219–239, 1970

Kopp, R.A., Holzer, T.E.: Dynamics of coronal hole regions. I. Steady polytropic flows with multiple critical points. Solar Phys. **49**, 43–56, 1976

Miggenrieder, H., Montgomery, M.D., Pilipp, W.G., Rosenbauer, H., Schwenn, R.: Preliminary results of the electron measurements in the solar wind by the HELIOS plasma experiment (abstract). EOS Trans. AGU **57**, 671, 1976

Montgomery, M.D., Gary, S.P., Feldman, W.C., Forslund, D.W.: Electromagnetic instabilities driven by unequal protons beams in the solar wind. J. Geophys. Res. **81**, 2743–2749, 1976

Montgomery, M.D., Gary, S.P., Forslund, D.W., Feldmann, W.C.: Electromagnetic ion-beam instabilities in the solar wind. Phys. Rev. Letters **35**, 667–670, 1975

Montgomery, M.D., Grünwaldt, H., Rosenbauer, H., Bame, S.J., Feldman, W.C.: Double ion streams in the solar wind: Correlations between HEOS-2 and IMP 6. Paper presented at the 16th International Conference, Comm. on Space Res., Konstanz, West Germany 1973

Pizzo, V., Hundhausen, A.J.: Nonradial motions in a hydrodynamic solar wind. EOS Trans. AGU **57**, 318, 1976

Rhodes, E.J., Smith, E.J.: Evidence of a large-scale gradient in the solar wind velocity. J. Geophys. Res. **81**, 2123–2134, 1976

Rosenbauer, H.: Possible effects of photo electron emission on a low energy electron experiment. In: Photon and particle interactions with surfaces in space, R.J.L. Grard and D. Reidel, eds., pp. 139–151. Dordrecht-Holland 1973

Rosenbauer, H., Miggenrieder, H., Montgomery, M., Schwenn, R.: Preliminary results of the HELIOS plasma measurements. In: Proc. of the AGU Intern. Symp. on Solar Terrestrial Phys., Boulder Colo. Donald J. Williams, ed., pp. 319–331, 1976a

Rosenbauer, H., Montgomery, M.D., Schwenn, R.: The characteristics of solar wind plasma emitted from coronal hole regions observed at 0.3 AU (abstract). EOS Trans. AGU **57**, 999, 1976b

Schwenn, R., Montgomery, M.D., Rosenbauer, H., Miggenrieder, H., Bame, S.J., Hansen, R.T.: The latitudinal extent of high speed streams in the solar wind: Correlations of HELIOS, IMP, and K-Corona measurements (abstract). EOS Trans. AGU **57**, 999, 1976

Schwenn, R., Rosenbauer, H., Miggenrieder, H.: Das Plasmaexperiment auf HELIOS (E1). Raumfahrtforschung **19**, 226–232, 1975

Sheeley, N.R., Jr., Harvey, J.W., Feldman, W.C.: Coronal holes, solar wind streams, and recurrent geomagnetic disturbances. Solar Phys. **49**, 271–278, 1976

Received March 24, 1977, Revised Version June 15, 1977